Cell, Vol. 83, 451–461, November 3, 1995, Copyright © 1995 by Cell Press

hemipterous Encodes a Novel Drosophila MAP Kinase Kinase, Required for Epithelial Cell Sheet Movement

Bruno Glise, Henri Bourbon, and Stéphane Noselli
Centre de Biologie du Développement
Unité Mixte de Recherche 9925
Centre National de la Recherche Scientifique
118, route de Narbonne
31062 Toulouse Cedex
France

Summary

During Drosophila embryogenesis, a cell sheet movement, dorsal closure, allows establishment of the dorsal epidermis. In this morphogenetic process, lateral epithelia undergo a dramatic movement toward the dorsal midline. In the mutant *hemipterous* (*hep*), spreading of the epithelia is blocked; in genetically sensitized *hep* embryos, cell sheet movement can be arrested at any time, indicating *hep* requirement in maintaining this morphogenetic activity. Further, *hep* is required for expression in the dorsal epithelium edges of another dorsal closure gene, *puckered*. The HEP protein is homologous to the Jun kinase kinase (JNKK) group of mitogen-activated protein kinase kinases (MAPKKs). These data suggest that *hep* functions in a novel Drosophila MAPK pathway, controlling *puckered* expression and morphogenetic activity of the dorsal epidermis.

Introduction

Morphogenetic movements play a central part in the establishment of germ layers and the overall body organization in metazoan development. The cellular and mechanistic aspects of concerted cell movements have been described in several organisms, and a number of studies suggest an important role for cell communication in morphogenesis (for reviews, see Fristrom, 1988; Hynes and Lander, 1992; Hynes, 1992; Costa et al., 1993). Yet, the molecular mechanisms underlying such fundamental cell behaviors remain poorly understood. In Drosophila, the identification of mutations affecting specific morphogenetic movements offers a means to identify gene pathways involved in these processes. One much-studied process is gastrulation, which involves folding and invagination of different cell sheets (for recent reviews, see Costa et al., 1993; Leptin, 1994).

In comparison, later morphogenetic processes taking place in multilayered and differentiated embryos have been less well characterized. In vertebrates, several pathologies have their origin in specific morphogenetic disorders (e.g., human dysraphism; Dias and Walker, 1992), demonstrating the importance of elaborating models of morphogenesis.

To develop a genetic model of cell sheet movement, we are investigating dorsal closure (DC) in Drosophila. DC takes place at midembryogenesis and allows the establishment of the dorsal epidermis (Campos-Ortega and Hartenstein, 1985; Martinez Arias, 1993). Before the onset of DC, only the ventral and lateral surfaces of the embryo are covered by epidermal cells, while the dorsal side is covered by the amnioserosa membrane. The main step in DC is the concerted, dorsalward spreading of the two lateral epidermal primordia over the amnioserosa. This movement is accompanied by epithelial cell elongation in the absence of either cell proliferation or cell rearrangement (Young et al., 1993). On meeting at the dorsal midline, the two cell sheets fuse and the internalized amnioserosa eventually degenerates. In contrast with our knowledge of the temporal and morphological hallmarks of DC, little is currently known about the molecules and, hence, the forces triggering and driving this morphogenetic movement. More particularly, it is unclear what mechanism(s) turns a motionless epithelium into a coordinated movable sheet of cells.

Near-saturation mutagenesis of the Drosophila genome provides an insight into DC by revealing a class of lethal mutations causing various defects in dorsal epidermis (Jürgens et al., 1984; Nüsslein-Volhard et al., 1984; Wieschaus et al., 1984; Perrimon et al., 1989). A prediction is that mutations altering DC genes should lead to embryonic lethality associated with defects in the formation of the dorsal epidermis and result in a dorsal hole. Such a phenotypic class could equally reflect alterations in the establishment of the dorsoventral axis (Terracol and Lengyel, 1994; Penton et al., 1994), so those mutants in which DC is selectively altered should be distinguished by virtue of their unaffected body plan.

We applied the above criteria to identify and clone a gene required specifically in DC, which we have named *hemipterous* (*hep*). Phenotypic analysis revealed that *hep* loss-of-function mutations impair DC, while the body plan remains unaffected. Embryos lacking both maternal and zygotic *hep* functions are blocked in the spreading phase of DC, thereby indicating that *hep* is important for proper morphogenetic activity of the cell sheets. Absence of epithelial motion in *hep* mutant embryos is accompanied by misexpression in the dorsal epithelium edges of an enhancer–trap inserted in *puckered* (*puc*), another DC gene (Ring and Martinez Arias, 1993). The predicted *hep* gene product is closely related to mitogen-activated protein kinase kinases (MAPKKs/MEKs; Ahn et al., 1992). We propose that epithelial morphogenetic activity during DC depends upon the activation of a novel MAPK-dependent signal transduction pathway in Drosophila, a candidate target of which is *puc*.

Results

Isolation of Mutations in the *hep* Locus

Mutations of genes with specific functions in DC are predicted to induce dorsal epidermal defects. We therefore focused on a P element–induced mutation that provokes such defects and that we have named hep^1. hep^1 is located

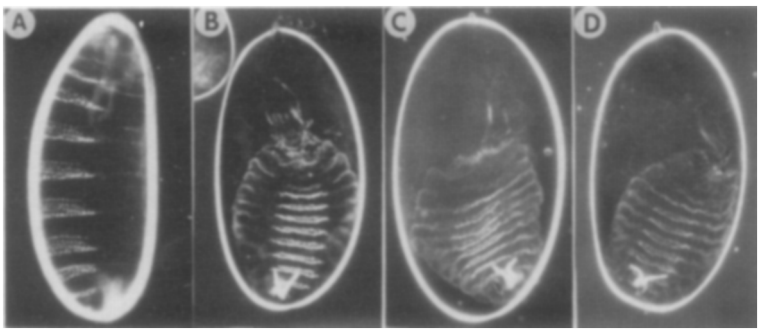

Figure 1. Cuticular Phenotype of *hep* Embryos

Dark-field photographs of cuticular preparations of a wild-type embryo (A) and of embryos derived from the following: homozygous hep^1/hep^1 females (B), heteroallelic hep^1/hep^{r75} females (C), and homozygous hep^{r75} germline clones (D). The embryos in (B)–(D) show a similar dorsal-open phenotype represented by lack of thoracic and abdominal dorsal cuticle. The head is very disorganized, with the cephalopharyngeal skeleton reduced to mouth hooks. The terminal structures, such as the posterior spiracles and Filzkörper, are normal. Anterior is top and posterior bottom. (A) is a lateral view; (B)–(D) are dorsal views.

on the X chromosome and is a recessive maternal effect mutation: homozygous hep^1 females crossed to hep^1 males lay eggs that do not hatch. In contrast, these females yield solely female progeny when mated to wild-type males, indicating that the paternal X chromosome can zygotically rescue the maternal effects of hep^1. In both crosses, cuticle preparations of dead embryos show a large gap in the dorsal structures (Figure 1B), suggesting that DC is abnormal (see below). In addition to a maternal effect, hep^1 causes poorly penetrant (~3%) but strikingly unilateral deletions of adult structures such as wing (hence the name of the gene), dorsal mesothorax, eye, or metathoracic leg (data not shown).

P element excisions generated by hybrid dysgenesis (see Experimental Procedures) led to two classes of revertants: 30 revertants behaved like wild type and presumably represent precise P excisions (see legend to Figure 5), whereas 4 resulted in a recessive, late larval/pupal lethality. These results establish that the hep^1 phenotypes are due to the X-linked P insertion. They also indicate that imprecise excisions of the transposon can generate a stronger, zygotic lethal phenotype. All four induced lethal mutations (referred to as hep^r) fail to complement the maternal effect of hep^1 (Figure 1C). Homozygous germline clones generated in hep^r/+ females (see Experimental Procedures) lead to embryos phenotypically similar to those derived from hep^1/hep^1 or heteroallelic hep^r/hep^1 females (Figure 1D). Together, these results indicate that hep^1 and hep^r mutations are allelic.

The single P[ry^+] insertion in hep^1 is located at cytological position 11D1,2. A previously identified mutation in the 11D interval, *l(1)7P1* (Perrimon et al., 1989), was tested and found to be allelic to hep^1. Deficiency mapping indicates that *Df(1)N12* uncovers the *hep* locus. Embryos from $Df(1)N12/hep^1$ females showed defects similar to those derived from hep^r/hep^1 females (data not shown), suggesting that hep^r alleles represent null or severely hypomorphic mutations. hep^1/hep^1 females also give rise to embryos phenotypically similar to heteroallelic combinations (Figure 1), suggesting that hep^1, although a viable allele, is a strong maternal effect but weak zygotic mutation.

hep Mutations Do Not Affect Axis Patterning

Although *hep* is required zygotically for larval/pupal development, we only focus here on its embryonic functions. Cuticles of mutant embryos derived from hep^1 homozygous females, heteroallelic mutant combinations, or hep^r germline clones (henceforth referred to as *hep* mutant embryos) display strong head defects and lack dorsal epidermis, resulting in a dorsal hole (Figures 1B–1D). A class of such mutations was revealed by extensive screening for embryonic lethal mutants (Jürgens et al., 1984; Nüsslein-Volhard et al., 1984; Wieschaus et al., 1984; Perrimon et al., 1989). These so-called dorsal-open mutants may represent a group of genes with specific functions in DC. Alternatively, this shared phenotype may also be due to incorrect patterning of the embryo at early stages, with dorsal epidermis defects appearing secondarily, e.g., as in the case of *thick veins* mutants (Nüsslein-Volhard et al., 1984; Terracol and Lengyel, 1994; Penton et al., 1994).

To examine whether inappropriate dorsoventral patterning might contribute to the dorsal opening of *hep* embryos, we analyzed the expression pattern of *Krüppel* (*Kr*) as a marker of the dorsal-most embryonic tissue, the amnioserosa (Ray et al., 1991).

From stages 1–12, i.e., before the onset of DC, the distribution of KR in *hep* embryos is indistinguishable from wild type, both spatially and temporally (Figures 2A and 2B; for a detailed description of embryogenesis, see Campos-Ortega and Hartenstein, 1985). The apparently normal development of *hep* embryos up to stage 13 was confirmed using anti-Engrailed (EN) antibodies (Figures 2C–2H) and other tissue-specific markers (data not shown). Two main conclusions can be drawn from these experiments. First, although *hep* mutations affect the fate of the dorsal region, the normal accumulation of the gap and segment polarity proteins KR and EN indicates that *hep* is not required for embryonic patterning. Second, the presence of an apparently unaffected amnioserosa indicates that the *hep* dorsal-open phenotype is probably not a consequence of inappropriate development of this tissue. In this respect, *hep* embryos differ from another dorsal hole mutant, *pannier*, in which amnioserosa cells die precociously or are absent, with dramatic consequences for DC (Ramain et al., 1993).

hep Embryos Fail to Undergo DC

The normal development of *hep* embryos up to stage 13 suggested that defects take place at later stages, i.e., during DC itself. To trace the dynamic changes that occur from stage 12 onward, we stained embryos with anti-EN

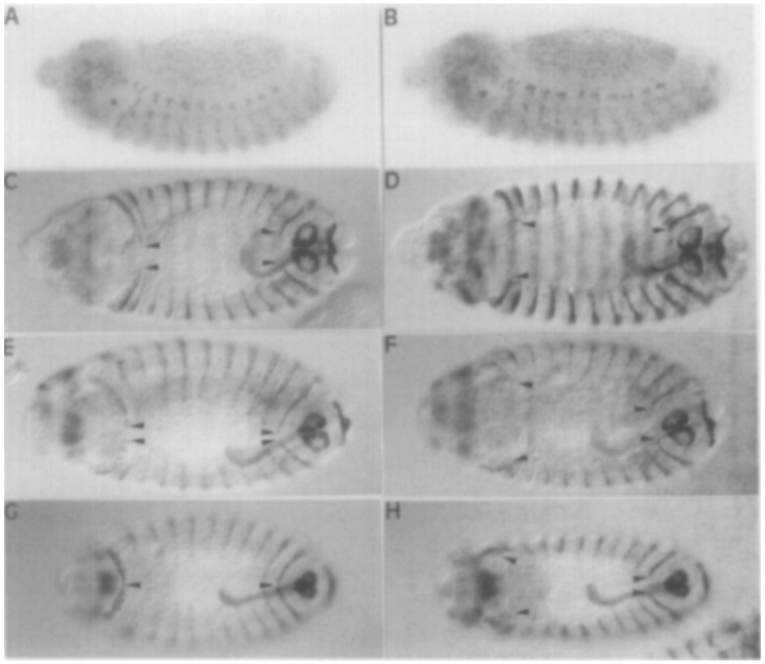

Figure 2. The Unaffected Body Plan and DC-Specific Defects of *hep* Embryos

Lateral views of wild-type (A) and *hep* (B) embryos labeled with anti-KR antibodies. In *hep* embryos, the distribution of KR is indistinguishable from wild type, and the overall morphologies are very similar. In these stage 13 embryos, DC has not yet begun, and the dorsal surface is covered by the amnioserosa sheet, easily recognizable due to its characteristic KR-expressing large nuclei. Dorsal views of wild-type (C, E, and G) and *hep* (D, F, and H) embryos labeled with anti-EN antibodies. The distribution of EN-expressing cells is similar in wild-type and mutant embryos, confirming that the body plan is unaffected in *hep* embryos. From stages 13–15, EN is expressed in epidermis as eleven stripes, thus enabling the movement of the epithelia to be traced during DC. The first difference observed between wild-type and *hep* embryos appears during stage 13 when the anterior- and posterior-most stripes, corresponding to the dorsal ridge and abdominal segment A7, respectively, move dorsalward (see arrowheads). While there is a conspicuous, increasingly accentuated dorsalward movement in the wild type (C, E, and G), in *hep* embryos no obvious migration of the lateral margins can be observed (D, F, and H). The consequence of the motionless *hep* phenotype is easily observed in stage 15 embryos (H), in which the EN stripes are still apart (and will stay so until the embryos die), while in the wild type, almost all thoracic and abdominal segments have met on dorsal midline and fused. Anterior is left.

antibodies, thus enabling the border between the amnioserosa and the epidermis to be visualized (Figures 2C–2H).

In the wild type, DC begins from the poles of the embryo and progresses gradually toward the center, the overall process lasting for about 2 hr (11–13 hr after egg laying; stage 13 to stage 15; Campos-Ortega and Hartenstein, 1985; Martinez Arias, 1993). A comparison of wild-type and *hep* embryos at different stages during DC indicates that the dorsalward migration of the lateral epithelia is defective in *hep* embryos. Detailed analysis reveals an initial epithelial movement in *hep* embryos (see below), whereas the characteristic long range spreading is overtly abolished (Figures 2C–2H). The anterior-most stripe of EN-expressing cells marks a gnathal-derived structure, the dorsal ridge, the formation of which relies on the fusion of its two lateral edges at the onset of DC (Figures 2C, 2E, and 2G; Campos-Ortega and Hartenstein, 1985). Once formed, the dorsal ridge slides anteriorly and delimits a dorsal fold, where head structures sink during head involution (stages 14–17). In contrast with the wild type, the dorsal ridge in *hep* embryos remains as a cleft as a consequence of the motionless phenotype (Figures 2D, 2F, and 2H). The absence of a functional dorsal ridge in *hep* embryos may well explain the disorganized head-derived cuticular structures (Figure 1), suggesting that the effect of *hep* mutations on the head involution process is indirect.

The spreading defect in *hep* embryos is always more pronounced in the anterior region (Figures 2F and 2H). We never observed the formation of the dorsal ridge, whereas the A7 posterior abdominal segment does, in some cases, close and fuse in hep^{1} embryos (but not in hep^{r75} embryos). This differential sensitivity may reflect regional variations in mechanical constraints. Indeed, slightly after the onset of DC, head involution induces dramatic reshaping of the anterior region, while in the posterior part, no such morphogenetic movement occurs.

In summary, *hep* embryos appear unable to extend the dorsal epidermal primordium slightly after DC has begun. The *hep* motionless phenotype seems to be restricted to the dorsal epidermal primordium, since ventral closure, for example, occurs normally (data not shown). These observations suggest that *hep* is specifically required for the DC process.

Epithelial Cell Shape Changes in *hep* Mutant Embryos

Cell elongation along the dorsoventral axis completely accounts for the approximately 3.5-fold gain in epidermal surface during DC (Young et al., 1993). Cell sheet movement is thus intimately linked to cell elongation, though it is unclear which event actually drives the other. Nevertheless, mutations in the DC genes *puc* (Ring and Martinez Arias, 1993) and *zipper* (Young et al., 1993) affect epithelial cell shape changes, thus enabling a correlation to be made between defects in DC and impaired cell elongation.

In early stage 13 wild-type embryos (fully retracted germband), the cells of the lateral epithelium have a characteristic polygonal shape (Figure 3A). The first changes occur during germband retraction, when the dorsal-most cells of the epithelium, the so-called leading edge, form a line and elongate along the dorsoventral axis (Figure 3A; Young et al., 1993; Ring and Martinez Arias, 1993; Martinez Arias, 1993). In *puc* mutant embryos, these cells do not become arranged in a straight line and do not elongate (Ring and Martinez Arias, 1993). In the wild type, cell elongation is restricted to the leading edge until germband

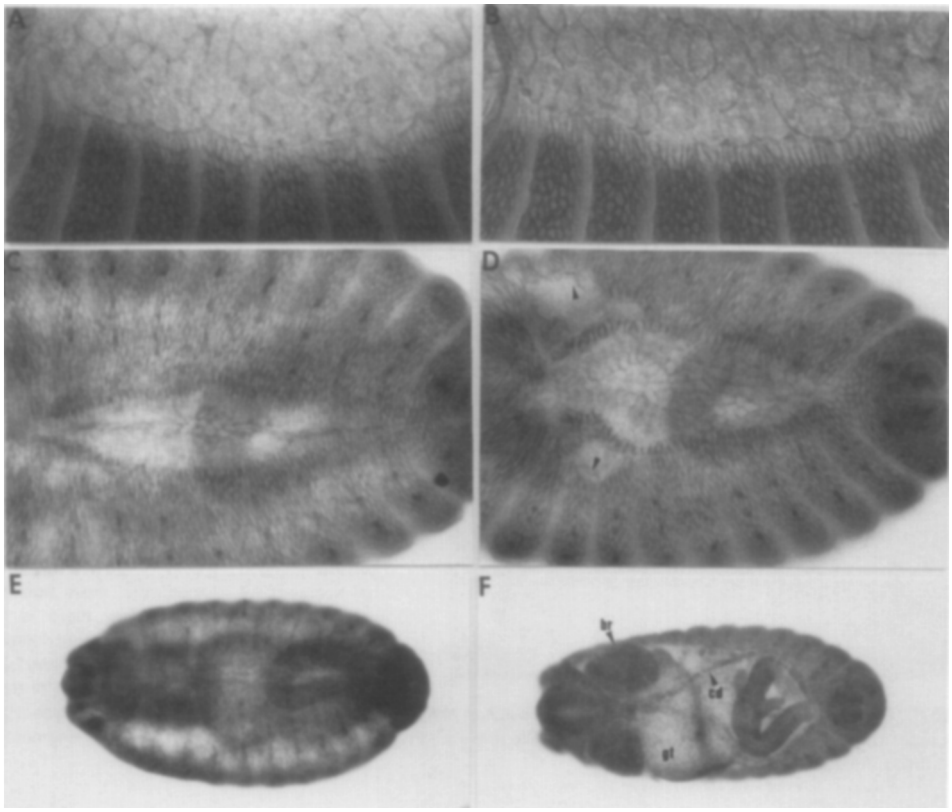

Figure 3. Epithelial Cell Shape Changes during DC in Wild-Type and *hep* Embryos

Wild-type (A, C, and E) and *hep* (B, D, and F) embryos have been labeled with anti-spectrin antibodies to reveal cell boundaries. (A) and (B) are lateral views, and (C)–(F) correspond to dorsal views. At the end of germband retraction, both wild-type (A) and *hep* (B) embryos display an elongation of the cells within the leading edge (see arrowheads), indicating that initiation of DC has taken place normally. At stage 15, slightly before the end of DC, wild-type embryos display characteristic dorsoventral elongated epidermal cells in both dorsal and lateral positions (C). In *hep* mutants (D), the leading edge is far from having reached the dorsal midline, and the cells are generally less elongated. In the embryo shown in (D), the four anterior-most segments have become detached from the amnioserosa and the resulting free epithelia have slackened, with the cells readopting a polygonal shape (D and F). When amnioserosa cells have totally degenerated, the dorsal surface is not covered, resulting in embryos with externalized organs (compare E and F). Anterior is left. cd, cardioblasts; br, brain; gt, gut.

retraction is completed, and only thereafter do the more ventral cells change shape, concomitantly with epithelium movement (Figure 3C). The cell shape changes occurring within the leading edge therefore represent a landmark for the initiation of DC.

The early events of DC, i.e., alignment and changes in shape of cells at the leading edge, do occur normally in *hep* mutant embryos (Figure 3B), suggesting that initiation of the process is correct. As DC continues, these cells stretch and their ventral neighbors also become elongated, indicating that the epithelium moves to some extent (Figure 3D). However, the leading edge then freezes in an intermediate position until what would normally be the end of DC (Figure 3D). At the end of stage 15, when DC is normally nearly completed (Figure 3C), both the lateral and leading edge cells of *hep* embryos appear less elongated (see Figure 3D). Once the amnioserosa begins to degenerate, the two lateral epithelia slacken ventrally and the cells readopt a polygonal shape (Figures 3D and 3F), in contrast with the complete elongation seen in the wild type (Figures 3C and 3E). As a consequence of the arrested movement, *hep* embryos lack a dorsal epidermis, and following complete amnioserosa degeneration, the organs such as gut, cardioblasts, and brain become externalized (Figure 3F).

hep Controls Gene Expression in the Leading Edge

As already mentioned, *puc* affects both the behavior of cells in the leading edge and the process of DC. In addition, an enhancer–trap inserted in *puc*, puc^{E69}, reveals a *lacZ* expression pattern restricted to the leading edge (Figure 4A; Ring and Martinez Arias, 1993). These observations thus make a strong case for a specific function of *puc*, and the leading edge, in DC.

Since the motionless phenotype in *hep* embryos can be interpreted as a blocking of the leading edge, we reasoned that *hep* mutations could modify cell fate in this part of the cell sheets. To test this assumption further, we compared the puc^{E69} *lacZ* expression in wild-type and *hep* embryos. In a *hep* mutant background, puc^{E69} *lacZ* expression in the margin is no longer observed (Figure 4B). The same result was obtained with another enhancer–trap line, *WG1173* (Bellen et al., 1989), whose expression pattern is also specific to the leading edge cells (data not shown).

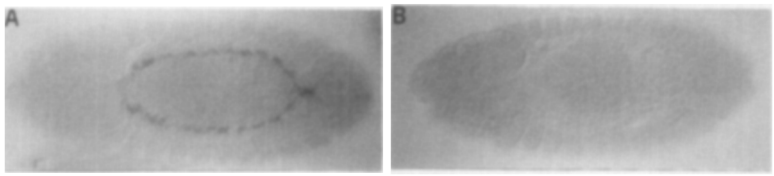

Figure 4. *hep* Controls Gene Expression in the Epithelium Leading Edge

Whole-mount X-Gal staining of wild-type (A) and *hep* (B) embryos (stage 13) containing one copy of the enhancer–trap line puc^{E69}. In wild-type embryos, β-galactosidase activity is detected in the cells of the leading edge. In contrast, in embryos mutant for *hep*, the staining is undetectable in these cells. Dorsal views. Anterior is left.

These data indicate that *hep* controls cell fate in the moving leading edge and that one function of *hep* during DC is to switch on specific gene expression in these cells.

Isolation of *hep* Sequences and Genetic Rescue

Genomic DNA flanking the P element in hep^1 was cloned by transposon tagging and used to isolate genomic λ phages and cDNAs. The genomic structures of the *hep* locus and of the five mutations described here are summarized in Figure 5. The P element in hep^1 is inserted 179 bp upstream of the ATG codon in the longest (2.2 kb) cDNA isolated (cDNA22). This, together with the DNA lesions associated with the four hep^r lethal revertants, suggests that cDNA22 corresponds to a *hep* cDNA.

To verify this assumption genetically, we constructed a chimeric *HShep* transgene placing the entire putative *hep* open reading frame present within cDNA22 (see below) under the control of the heat-inducible *hsp70* promoter. The basal expression level of *HShep* is sufficient to rescue the maternal effect of *hep* mutations (Figure 6B), confirming that cDNA22 corresponds to *hep*. This result was confirmed using a ubiquitin promoter–*hep* cDNA22 transgene (*UBhep*), which allows complete rescue of both the DC maternal effect and zygotic lethality. Interestingly, in the *HShep* experiments, a small proportion of embryos were only partially and variably rescued, undergoing DC to variable extents (Figures 6C and 6D; see Discussion). Partial closure was not observed with *UBhep* constructs, indicating that it is due to limiting amounts of *hep* function provided by uninduced *HShep*.

The analysis of the temporal distribution of *hep* transcripts in Northern blot experiments revealed an mRNA of approximately 6 kb present throughout development (data not shown). Hence cDNA22, while carrying all *hep* functions as revealed by rescue experiments, is not full length and lacks some untranslated sequences.

In contrast with the specific effects of *hep* mutations in DC, in situ hybridization to whole-mount embryos using cDNA22 as a probe revealed a homogeneous distribution of *HEP* mRNAs (data not shown).

hep Encodes a Novel MAPKK/MEK Homolog

The complete nucleotide sequence of cDNA22 and of an additional 515 bp in the 3′ region was determined (Figure 7A). The predicted *hep* gene product (HEP) is 487 amino acids long, and database searches revealed a significant homology to members of the MAPKK/MEK protein kinase family (for review, see Ahn et al., 1992). As shown in Figure 7B, HEP and other MAPKK catalytic domains display from 39% to 56% overall amino acid identity (54% to 68% similarity). More particularly, the two known phosphorylation sites required for MAPKK activation are well conserved in HEP (Figure 7B; Alessi et al., 1994; Zheng and Guan, 1994). Based on the presence or the absence of an insertion between the kinase subdomains IX and X, two MAPKK subgroups are distinguished (Figure 7B). As reported recently, this subdivision appears functionally relevant, since different human MEKs show a selective specificity for various MAPK subtypes (Dérijard et al., 1995). HEP, like its closest human (MKK3 and MKK4; Dérijard et al., 1995) and Xenopus (XMEK2; Yashar et al., 1993) homologs, does not possess such an insertion and, thus, likely represents a Drosophila homolog of the JNKK family of MAPKK (Dérijard et al., 1995; Lin et al., 1995).

The prediction that *hep* encodes a protein kinase was assessed biochemically. A purified glutathione S-transferase (GST)–HEP fusion protein (Smith and Johnson, 1988; see Experimental Procedures) undergoes autophosphorylation, as reported previously for vertebrate MEKs (Kosako et al., 1993; Zheng and Guan, 1993), although poorly compared with a MAPK (Figure 7C). The absence

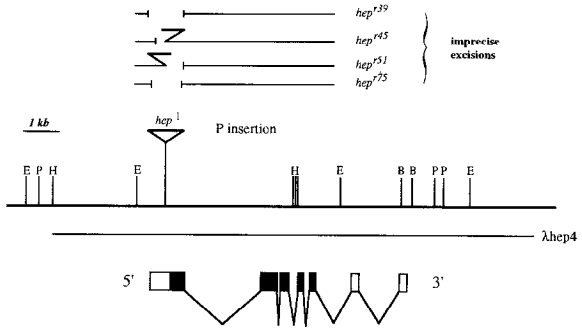

Figure 5. Molecular Organization of the *hep* Locus

Genomic organization of the *hep* locus and of a composite 2.7 kb cDNA. The triangle symbolizes the position of the P element in the hep^1 strain. The lines above the restriction map indicate the DNA lesions associated with four hep^r alleles, as determined by Southern blot analysis. In contrast, no genomic aberrations were detected in two wild-type revertants, confirming that this class of revertants arises from precise excisions. The broken lines indicate DNA deletions in the 6 kb EcoRI fragment encompassing the cDNA, while the truncated triangles in hep^{r45} and hep^{r51} indicate partial excisions of the hep^1 P element. Below the restriction map is indicated one recombinant phage (λhep4) isolated from the *hep* region and the structure of the composite *hep* cDNA. Broken lines indicate the introns, and the solid boxes represent the coding region. Restriction sites are abbreviated as follows: E, EcoRI; B, BamHI; H, HindIII; P, PstI.

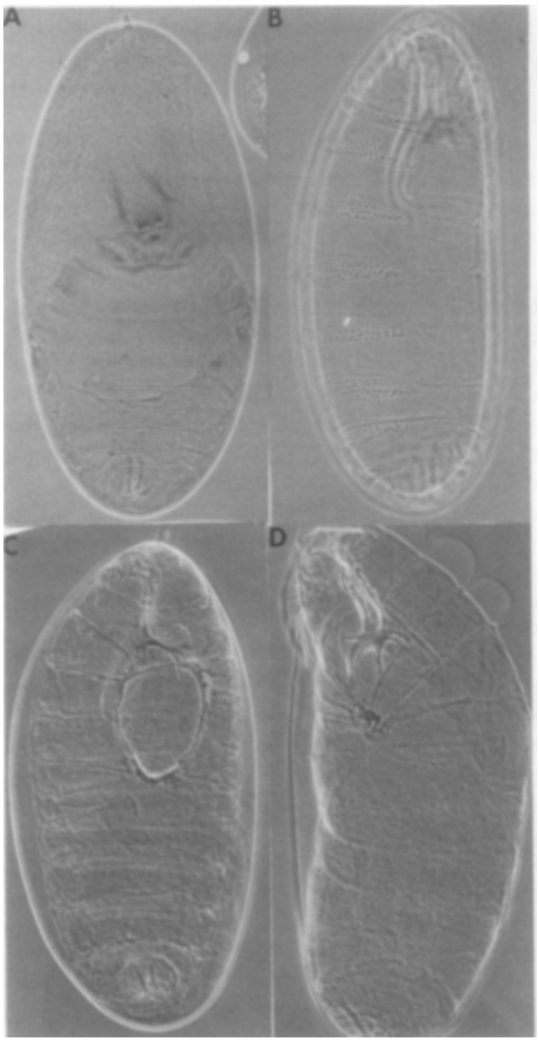

Figure 6. Rescue of the Cell Sheet Spreading Defects with an *HShep* Transgene

Phase-contrast cuticular phenotype of embryos derived from homozygous germline clones generated in *y w hep^{r75} FRT101/w ovo^{D1} v^{24} FRT101*; *FLP38/+* females crossed to wild-type males (A), or to transgenic males homozygous for an *HShep* construct on the third chromosome (B–D). In the absence of heat shock, most embryos are fully rescued and develop normally (B), while a minority (~2%) display DC to a variable extent (C and D), as illustrated by the variable hole size on the dorsal side. (A), (C), and (D) are dorsal views; (B) is a lateral view.

of autophosphorylation of purified GST on its own indicates that the kinase activity depends strictly upon the HEP sequences (data not shown). The GST–HEP kinase activity is abolished in a deletion mutant removing the entire HEP kinase domain (GST–HEPΔK; Figure 7C). Taken together, the structural and biochemical data strongly suggest that *hep* encodes a protein kinase of the MEK family.

Discussion

We report here that *hep* is required for DC of the Drosophila embryo. Specifically, embryos lacking both maternal and zygotic *hep* functions initiate but fail to complete DC, resulting in a characteristic dorsal-open phenotype. Several lines of evidence indicate that these developmental defects are due to dysfunction of a novel Drosophila MAPKK protein encoded by the *hep* locus. First, all five *hep* alleles described here carry DNA lesions within the *hep* locus. Second, expression of either *HShep* or *UBhep* transgenes is able to rescue the DC defects associated with *hep* mutations. Finally, structural homology of the predicted *hep* gene product with MAPKK proteins and the ability of HEP to undergo autophosphorylation in vitro are consistent with *hep* encoding a novel Drosophila MAPKK homolog.

These data suggest that *hep* participates in a MAPK pathway, which we refer to below as the DC signal transduction pathway.

A Novel MAPK Pathway in Drosophila

In a number of organisms, including yeast, nematode, and human, multiple gene isoforms for components of the MAPK pathway have been identified. This has led to the general idea that eukaryotic cells use related, but functionally different, MAPK pathway "modules" (Davis, 1994; Herskowitz, 1995). In yeast, six distinct MAPK pathways have been identified that control, for example, mating, response to changes in osmolarity, or cell wall integrity (Blumer and Johnson, 1994; Herskowitz, 1995). In Drosophila, only one MAPK pathway has been identified so far, and it is the focus of intense genetic and molecular analysis (for review, see Perrimon, 1994; Dickson and Hafen, 1994). In contrast with the situation in yeast, this pathway was shown to transduce signals received from at least three different receptor tyrosine kinases (RTKs), encoded by the genes *torso* (*tor*), the *Drosophila EGF receptor* homolog (*DER*), and *sevenless* (*sev*); the three Drosophila RTKs act in different tissues and/or at different developmental stages to specify the embryonic termini, the dorsoventral polarity, and the fate of the R7 photoreceptor in the compound eye, respectively. Because the same Drosophila MAPKK gene (*Dsor1*; Tsuda et al., 1993) and the same ERK gene (*rolled*; Biggs et al., 1994; Brunner et al., 1994) participate in all three pathways, it was suggested that they could represent RTK-specific signal transducers (Hsu and Perrimon, 1994). The identification of *hep* now strongly indicates that, in addition to the above pathways, at least one additional MAPK pathway acts in Drosophila development to control DC. Three independent observations indicate that *hep* participates in a different, and therefore novel MAPK pathway. First, sequence comparison between HEP and DSOR1 indicate that they belong to two functionally separate MEK subgroups, suggesting that they activate different MAPK substrates (Davis, 1994; Dérijard et al., 1995; Lin et al., 1995). Second, several genetic screens failed to identify *hep* as a modifier of the *rolled* (MAPK) pathway, whereas alleles of *Dsor1* were isolated by this procedure (Tsuda et al., 1993; Lu et al., 1994). Finally, we have tested directly the potential suppressor activity of a *rolled* gain-of-function mutation, *Sevenmaker* (*Sem*), in *hep* mutant embryos. Whereas *Sem* suppresses

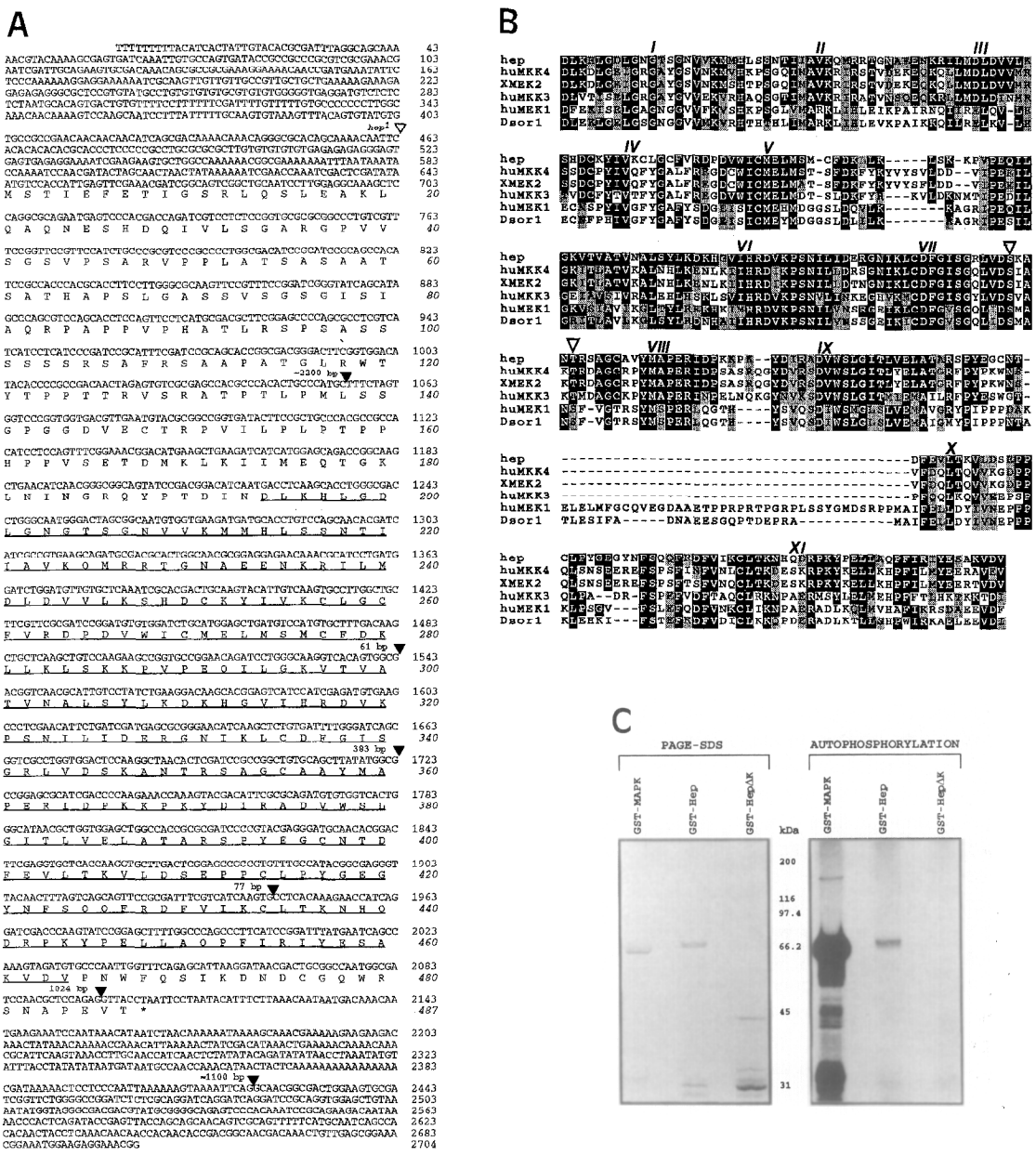

Figure 7. Nucleotide and Protein *hep* Sequences and the Ability of HEP Protein to Autophosphorylate

(A) Nucleotide sequence of a composite *hep* cDNA and deduced amino acid sequence. The catalytic domain is underlined. The positions (closed triangles) and sizes of introns are given. The P element in *hep'* is inserted at position 464 in the 5' mRNA leader (open triangle).

(B) Sequence alignment of HEP and other MEK catalytic domains using the CLUSTALV alignment program. Hep, Drosophila Hemipterous; huMKK3, human MKK3; huMKK4, human MKK4 (Dérijard et al., 1995); XMEK2, Xenopus laevis MEK2 (Yashar et al., 1993); huMEK1, human MEK1 (Seger et al., 1992); Dsor1, Drosophila suppressor of D-raf (Tsuda et al., 1993). The two sites of activating phosphorylation in MEK are indicated by open arrowheads. Division into subdomains I–XI is according to Hanks et al. (1988). Gaps introduced to optimize the alignment are represented by dashes. Identical residues are indicated by a black background, while similar amino acids are in stippled. The identity and similarity of MEK with HEP were calculated to be as follows (percent identity to percent similarity): huMKK4, 56%/68%; XMEK2, 56%/66%; huMKK3, 48%/62%; huMEK1, 40%/58%; DSOR1, 40%/57%.

(C) Autophosphorylation of HEP. Purified GST–MAPK, GST–HEP (GST–Hep), and GST–HEPΔK (GST–HepΔK) fusion proteins were incubated in the presence of radiolabeled ATP, run on an SDS–polyacrylamide gel, and autoradiographed. The autophosphorylation of GST–HEP depends on the C-terminal kinase domain, since a construct with a deleted domain (GST-HEPΔK) is no longer able to autophosphorylate.

upstream loss-of-function mutations in the *tor* and *sev* pathways (Brunner et al., 1994), it is unable to suppress, even partly, the DC defects observed in *hep* embryos (data not shown). Both results indicate that HEP and Rolled do not participate in the same pathways during Drosophila embryogenesis. We suggest that another as yet unidentified MAPK exists in Drosophila, which acts in the DC pathway.

Role of *hep* in DC

The behavior of epidermal cells during DC is well documented in wild-type embryos and in a few mutant backgrounds (Young et al., 1993; Ring and Martinez Arias, 1993; Martinez Arias, 1993; Fehon et al., 1994). Both from these studies and from our observations, the DC process in each segmental unit can be schematically divided into three steps: initiation, i.e., determination of the epithelium as morphogenetically competent; spreading, which consists of the coordinate dorsalward movement of the two lateral epithelia; suture of the convergent epithelia at the dorsal midline. We present evidence here that *hep* mutations specifically block spreading, a phenotype not previously described. In contrast with *puc* (Ring and Martinez Arias, 1993), our data suggest that *hep* is not required for the initiation phase. Conversely, since *hep* embryos do not close, we cannot exclude the possibility that *hep* also plays a role in the suture of epithelia at the dorsal midline.

What is the role of *hep* in cell sheet spreading? Careful inspection of *hep* embryos suggests that spreading proceeds in two separate phases, one *hep*-independent and the other not. The initial short-range movement of the epithelium observed in *hep* embryos may reflect a morphogenetic activity of the epithelium independent of *hep* function. But, since none of the *hep* mutations studied here is a confirmed null allele, this apparently intrinsic morphogenetic activity may also be due to some residual *hep* function. In a second phase, however, *hep* is clearly required for the displacement of the epithelium margin from an intermediate position to its final location, at the dorsal midline. As a whole, this process lasts for about 2 hr, and an important question is how *hep* works during this phase: i.e., is it necessary to trigger the movement, or is it rather required during the process? One way to address this question is to sensitize embryos by providing them with threshold amounts of the *hep* product, as in our rescue experiments using *HShep*. While most embryos were rescued, a small proportion displayed variable degrees of incomplete DC, as illustrated by the variable size of their dorsal hole (Figure 6). That DC aborted at different intermediate stages strongly suggests that *hep* is required for maintenance of the morphogenetic activity of the epidermal epithelium. Indeed, if *hep* were only a trigger for cell sheet movement, one should not observe embryos with some, but not all, segmental units fused.

Although *hep* is clearly crucial for correct spreading, it is not clear which cell type(s) requires its function. The gene is uniformly expressed in embryos, and it is not possible to correlate this pattern with any localized requirement. However, we show here that the *hep* motionless phenotype is accompanied by misexpression in the margin of the puc^{E69} enhancer–trap. This finding therefore represents strong evidence that *hep* function is required in the leading edge. The question of whether *hep* is specifically required in the margin could be addressed further using the GAL4 system to direct *hep* expression in these cells during DC (Brand and Perrimon, 1993). The requirement of hep^{+} for normal puc^{E69} expression reinforces the notion of a particular status of the leading edge (Martinez Arias, 1993) and suggests that this line of cells is crucial in the displacement of the entire cell sheet toward the dorsal midline.

Based on our data, the role of *hep*, and the postulated DC signal transduction pathway, can be viewed as a switch between two alternative cell sheet behaviors. In this view, signaling via *hep* is sufficient to convert the motionless dorsal epidermal primordium to a movable entity. This behavior appears to be reversible in embryos with limiting amounts of *hep*, in which the cell sheets become fixed again. This switch model predicts that the initiation/spreading and spreading/suture transitions may correspond to the turning on and off of the DC signaling pathway, respectively, and that the activity of the putative DC signal might fit these variations.

Control of Cell Sheet Movement by a MAPK Pathway

We show here that concerted cell sheet movement requires signaling via a novel MEK, thus providing a link between this morphogenetic process and MAPK pathways. This finding suggests for DC a signal transduction mechanism similar to that shared by other known MAPK pathways (Blumer and Johnson, 1994; Herskowitz, 1995).

Few target genes of the MAPK pathways have been identified in metazoa. In the Drosophila *tor* pathway, expression of the *tailless* gene is regulated at embryonic termini (Tsuda et al., 1993), while *phyllopod*, which encodes a novel nuclear protein, has been recently identified as the first immediate transcriptional target of the *sev* pathway in the Drosophila retina (Dickson et al., 1995; Chang et al., 1995). The *hep*-dependent activation of puc^{E69} expression in the cells of the leading edge makes *puc* a good candidate for a downstream genomic target of the DC pathway, a possibility that can now be examined at the level of *PUC* mRNA expression. The differences observed between *puc* (Ring and Martinez Arias, 1993) and *hep* DC initiation phenotypes suggest in turn that *hep* may induce other cell responses apart from the control of *puc* gene expression. The other so far identified genes with a demonstrated function in DC encode a β-integrin subunit (*l(1)myospheroid;* MacKrell et al., 1988), nonmuscle myosin heavy chain (*zipper*; Young et al., 1993), a Drosophila homolog of the 4.1 vertebrate membrane-skeletal protein (*coracle*; Fehon et al., 1994), and a transcriptional regulator homologous to vertebrate GATA-1 (*pannier*; Ramain et al., 1993; Winick et al., 1993), suggesting critical roles for the cytoskeleton, cell adhesion, and as shown here, the control of gene expression in the process of DC. However, although these proteins are clearly involved in several aspects of epithelial and amnioserosa cell function, their participation in a common pathway remains to be established. Undoubtedly, the characterization of additional DC genes among those affecting the formation of the dorsal epidermis, in combination with screens for genetic modifiers of *hep*, will help to identify the molecules that cooperate in the DC morphogenetic process and should provide answers to some of the following questions. How are the cytoskeleton and cell adhesion molecules connected to MAPK pathways in cell movement? Does the DC signal transduction

pathway share components with other well studied pathways? And finally, have the mechanisms of cell sheet movement in Drosophila been conserved during evolution?

Experimental Procedures

Genetics

A description of genetic markers and chromosome balancers used in this study can be found in Lindsley and Zimm (1992). The P element *hep*^{1} mutation was isolated from a *ry*^{506} stock transformed by a P[*ry*$^{+}$; *sry–lacZ*] transposon (Noselli et al., 1992).

The P insertion in *hep*^{1} was mobilized by providing an external source of P transposase, and excisions were selected through the loss of the *ry*$^{+}$ marker. Of the 34 excision lines tested, 4 (*hep*^{r39}, *hep*^{r45}, *hep*^{r51}, and *hep*^{r75}) bore an X-linked larval lethality.

Homozygous germline clones for *hep*^{r} mutations were induced by mitotic recombination using the FLP–DFS technique (Chou and Perrimon, 1992). The progeny of *y w hep*^{r} *FRT101/FM6*; +/+ females crossed to *w ovo*^{D1} *v*^{24} *FRT101/Y*; *FLP38/FLP38* males were heat shocked (37°C) for 1 hr at pupal stage to induce mitotic recombination. Then, *y w hep*^{r} *FRT101/w ovo*^{D1} *v*^{24} *FRT101*; *FLP38/+* females were mated to Oregon-R wild-type males. The progeny were allowed to develop for 1 day at 22°C, before collecting dead embryos for observation of cuticles as previously described (Wieschaus and Nüsslein-Volhard, 1986).

Isolation and Sequence of Genomic and cDNA Clones

Handling of phages and DNA and library screenings followed standard methods (Sambrook et al., 1989). To isolate sequences flanking the P[*ry*$^{+}$] element in *hep*^{1}, genomic DNA was double digested with PstI and NcoI to make a size-selected library in a plasmid derived from pSP64 (Promega). Screening with a probe corresponding to the 3′ end of the P element identified clones containing 9 kb of genomic DNA. This insert was subsequently used as a probe to isolate several clones from a λCharon4 genomic library (Maniatis et al., 1978). The λhep4 phage, which encompasses the *hep*^{1} P insertion, was finally used to isolate cDNAs from staged 8–12 hr and 12–24 hr embryonic libraries (Brown and Kafatos, 1988). To isolate additional 3′ sequences, we performed RT–PCR cloning experiments using forward (5′-CCTAATTCCTAATACCATTTC-3′) and reverse (5′-CCGTTTCCTCTTCCATTTCC-3′) primers, which hybridize to positions 2103–2123 and 2674–2693 in the cDNA sequence, respectively. Reverse primer is included in a 342 bp BamHI genomic fragment located 1.5 kb to the 3′ end of cDNA22 and hybridizing to *hep* transcripts in Northern blot experiments. Comparison of the size of PCR products generated from cDNA and genomic DNA indicates the presence of an approximately 1.1 kb intron.

The nucleotide sequence of the composite 2.7 kb cDNA was determined on both DNA strands by dideoxy sequencing using Sequenase (United States Biochemical Corporation). The *hep* genomic DNA was partly sequenced on one strand to map intron/exon boundaries. Introns 2, 3, 4, 5, and approximately 90% of sequences contained in the cDNA were sequenced from genomic DNA. The cDNA and relevant genomic fragments were subcloned and sequenced after clones with a series of deletions were produced using ExoIII nuclease (Sambrook et al., 1989).

Genetic Rescue Experiments

The *HShep* construct was made by introducing cDNA22 (nucleotides 1–2189 in Figure 1) fragment bordered by BamHI and XbaI restriction sites into the BglII and XbaI sites of the transformation vector pCaSpeR-HS (Thummel and Pirrotta, 1992). The *UBhep* construct was made by introducing a 4.5 kb NotI fragment containing ubiquitin promoter–(2.1 kb fragment obtained from plasmid RHXpHSS7-Up2; provided by R. Fehon)–*hep* cDNA22–*hsp70* 3′ UTR region into the NotI site of the pCaSpeR4 transformation vector (Thummel and Pirrotta, 1992). Four independent *HShep* lines were tested, and all rescued *hep* embryos without heat shock. Three independent *UBhep* lines were tested and rescued DC defects and zygotic lethality. To test rescue of DC defects, either homozygous *hep*^{1} females or homozygous germline clones generated in *y w hep*^{r75} *FRT101/w ovo*^{D1} *v*^{24} *FRT101*; *FLP38/+* females were crossed to males carrying either homozygous or balanced *HShep* or *UBhep* constructs. Cuticle preparations of dead embryos were performed as described above. Rescue of the zygotic lethality was assessed by checking *y w hep*^{r}*/Y*; P[*UBhep*; mini-*w*$^{+}$]/+ adult males in the progeny of *y w hep*^{r}*/FM6*; +/+ females mated to *w/Y*; P[*UBhep*; mini-*w*$^{+}$]*/TM3*, *Sb* or P[*UBhep*; mini-*w*$^{+}$]*/CyO* males.

Immunocytochemistry and X-Gal Staining

Unless otherwise noted, stainings were performed on the phenotypically homogeneous progeny of *hep*^{1}*/hep*^{1} females mated to *hep*^{1} males. Whole-mount antibody staining of staged embryos was performed as described by Ashburner (1989), and revelation was done using the HRP ABC kit (Vectastain). For X-Gal stainings, *hep*^{1}*/hep*^{1} females were mated to either *hep*^{1}*/Y*; *WG1173/+* or *hep*^{1}*/Y*; *puc*^{E69}*/+* males and allowed to lay eggs for 15 hr. Then, embryos were collected and stained for β-galactosidase activity according to standard protocols (Ashburner, 1989).

Protein Purification and Kinase Assays

The vector pGST-MAPK expressing a recombinant Chinese hamster GST-p44^{MAPK} was a gift of J. Pouysségur. The pTPVE plasmid was constructed by restricting pTZ18R with SmaI and EcoRI and inserting a 1.5 kb PvuI (blunted with T4 DNA polymerase)–EcoRI fragment from cDNA22. To create pGST–HEP, pGEX-B (Valle et al., 1992) was restricted with BamHI and EcoRI and ligated with a BamHI–EcoRI fragment from pTPVE, fusing in-frame GST to the entire *hep* ORF except the first ten amino acids. pGST–HEPΔK was constructed by internal deletion of the kinase domain in pGST–HEP plasmid cut with EagI and EcoRI, treated with Klenow, and self-ligated. Expression and purification of various GST fusion proteins followed the technique described by Smith and Johnson (1988). Protein kinase assays were done in kinase buffer as described by Kosako et al. (1993). The reactions were terminated after 30 min at 37°C by addition of Laemmli sample buffer. Autophosphorylation was examined after SDS–polyacrylamide gel electrophoresis (SDS–PAGE) by autoradiography.

Acknowledgments

Correspondence should be addressed to S. N.; B. G. and S. N. contributed equally to this work. This study was initiated in the laboratory of A. Vincent, and we thank him for his generous support. We wish to thank T. B. Chou, C. Coyle-Thompson, E. Hafen, A. Martinez Arias, Y. Nishida, C. Nüsslein-Volhard, N. Perrimon, M. Sémériva, and the Umea and Bloomington stock centers for Drosophila stocks. We are grateful to C. Benassayag, S. Brand, N. Brown, R. Fehon, D. Kiehart, M. Levine, J. Pouysségur, and T. Maniatis for providing various materials and reagents. We thank A. Martinez Arias and Y. Nishida for communicating unpublished results. We also thank D. Cribbs, P. Simpson, J. Smith, and A. Vincent for comments on the manuscript and members of the laboratory for discussions. B. G. is supported by the Ministère de l'Enseignement Supérieur et de la Recherche. This work is supported by the Centre National de la Recherche Scientifique and by the Association pour la Recherche contre le Cancer (grant 1184).

Received May 9, 1995; revised September 18, 1995.

References

Ahn, N.G., Seger, R., and Krebs, E.G. (1992). The mitogen-activated protein kinase activator. Curr. Opin. Cell Biol. *4*, 992–999.

Alessi, D.R., Saito, Y., Campbell, D.G., Cohen, P., Sithanandam, G., Rapp, U., Ashworth, A., Marshall, C.J., and Cowley, S. (1994). Identification of the sites in MAP kinase kinase-1 phosphorylated by p74^{raf-1}. EMBO J. *13*, 1610–1619.

Ashburner, M. (1989). *Drosophila*: A Laboratory Manual (Cold Spring Harbor, New York: Cold Spring Harbor Laboratory Press).

Bellen, H.J., O'Kane C.J., Wilson, C., Grossniklaus, U., Pearson, R.K., and Gehring, W.J. (1989). P-element mediated enhancer detection: a versatile method to study development in *Drosophila*. Genes Dev. *3*, 1288–1300.

Biggs, W.H., III, Zavitz, K.H., Dickson, B., van der Straten, A., Brunner,

D., Hafen, E., and Zipursky, S.L. (1994). The *Drosophila rolled* locus encodes a MAP kinase required in the *sevenless* signal transduction pathway. EMBO J. *13*, 1628–1635.

Blumer, K.J., and Johnson, G.L. (1994). Diversity in function and regulation of MAP kinase pathways. Trends Biochem. Sci. *19*, 236–240.

Brand, A.H., and Perrimon, N. (1993). Targeted gene expression as a means of altering cell fates and generating dominant phenotypes. Development *118*, 401–415.

Brown, N.H., and Kafatos, F.C. (1988). Functional cDNA libraries from *Drosophila* embryos. J. Mol. Biol. *203*, 425–437.

Brunner, D., Oellers, N., Szabad, J., Biggs, W.H., III, Zipursky, S.L., and Hafen, E. (1994). A gain-of-function mutation in Drosophila MAP kinase activates multiple receptor tyrosine kinase signaling pathways. Cell *76*, 875–888.

Campos-Ortega, J.A., and Hartenstein, V. (1985). The Embryonic Development of *Drosophila melanogaster* (Berlin: Springer-Verlag).

Chang, H.C., Solomon, N.M., Wassarman, D.A., Karim, F.D., Therrien, M., Rubin, G.M., and Wolff, T. (1995). *phyllopod* functions in the fate determination of a subset of photoreceptors in Drosophila. Cell *80*, 463–472.

Chou, T.-B., and Perrimon, N. (1992). Use of a yeast site-specific recombinase to produce female germline chimeras in *Drosophila*. Genetics *131*, 643–653.

Costa, M., Sweeton, D., and Wieschaus, E. (1993). Gastrulation in *Drosophila*: cellular mechanisms of morphogenetic movements. In The Development of *Drosophila*, M. Bate and A. Martinez Arias, eds. (Cold Spring Harbor, New York: Cold Spring Harbor Laboratory Press).

Davis, J.D. (1994). MAPKs: new JNK expands the group. Trends Biochem. Sci. *19*, 470–473.

Dérijard, B., Raingeaud, J., Barret, T., Wu, I.-H., Han, J., Ulevitch, R. J., Davis, R. (1995). Independent human MAP kinase signal transduction pathways defined by MEK and MKK isoforms. Science *267*, 682–685.

Dias, M.S., and Walker, M.L. (1992). The embryogenesis of complex dysraphic malformations: a disorder of gastrulation? Pediatr. Neurosurg. *18*, 229–253.

Dickson, B., and Hafen, E. (1994). Genetics of signal transduction in invertebrates. Curr. Opin. Genet. Dev. *4*, 64–70.

Dickson, B.J., Domínguez, M., van der Straten, A., and Hafen, E. (1995). Control of Drosophila photoreceptor cell fates by phyllopod, a novel nuclear protein acting downstream of the Raf kinase. Cell *80*, 453–462.

Fehon, R.G., Dawson, I.A., and Artavanis-Tsakonas, S. (1994). A *Drosophila* homologue of membrane-skeleton protein 4.1 is associated with septate junctions and is encoded by the *coracle* gene. Development *120*, 545–557.

Fristrom, D. (1988). The cellular basis of epithelial morphogenesis: a review. Tissue Cell *20*, 645–690.

Hanks, S.K., Quinn, A.M., and Hunter, T. (1988). The protein kinase family: conserved features and deduced phylogeny of the catalytic domains. Science *241*, 42–52.

Herskowitz, I. (1995). MAP kinase pathways in yeast: for mating and more. Cell *80*, 187–197.

Hsu, J.C., and Perrimon, N. (1994). A temperature-sensitive MEK mutation demonstrates the conservation of the signaling pathways activated by receptor tyrosine kinases. Genes Dev. *8*, 2176–2187.

Hynes, R.O. (1992). Integrins: versatility, modulation, and signaling in cell adhesion. Cell *69*, 11–25.

Hynes, R.O., and Lander, A.D. (1992). Contact and adhesive specificities in the associations, migrations, and targeting of cells and axons. Cell *68*, 303–322.

Jürgens, G., Wieschaus, E., Nüsslein-Volhard, C., and Kluding, H. (1984). Mutations affecting the pattern of the larval cuticle in *Drosophila melanogaster* II. Zygotic loci on the third chromosome. Roux's Arch. Dev. Biol. *193*, 283–295.

Kosako, H., Nishida, E., and Gotoh, Y. (1993). cDNA cloning of MAP kinase kinase reveals kinase cascade pathways in yeasts to vertebrates. EMBO J. *12*, 787–794.

Leptin, M. (1994). Control of epithelial cell shape changes. Curr. Biol. *4*, 709–712.

Lin, A., Minden, A., Martinetto, H., Claret, F., Lange-Carter, C., Mercurio, F., Johnson, G.L., and Karin, M. (1995). Identification of a dual specificity kinase that activates the Jun kinases and P38–Mpk2. Science *268*, 286–290.

Lindsley, D.L., and Zimm, G.G. (1992). The Genome of *Drosophila melanogaster* (San Diego: Academic Press).

Lu, X., Melnick, M.B., Hsu, J.C., and Perrimon, N. (1994). Genetic and molecular analyses of mutations involved in *Drosophila* raf signal transduction. EMBO J. *13*, 2592–2599.

MacKrell, A.J., Blumberg, B., Haynes, S.R., and Fessler, J.H. (1988). The lethal *myospheroid* gene of *Drosophila* encodes a membrane protein homologous to vertebrate integrin β subunits. Proc. Natl. Acad. Sci. USA *85*, 2633–2637.

Maniatis, T., Hardison, R.C., Lacy, E., Lauer, J., O'Connell, C., Quon, D., Sim, G.K., and Efstratiadis, A. (1978). The isolation of structural genes from libraries of eucaryotic DNA. Cell *15*, 687–701.

Martinez Arias, A. (1993). Development and patterning of the larval epidermis of *Drosophila*. In the Development of *Drosophila melanogaster*, Volume I, M. Bate and A. Martinez Arias, eds. (Cold Spring Harbor, New York: Cold Spring Harbor Laboratory Press), pp. 517–608.

Noselli, S., Payre, F., and Vincent, A. (1992). Zinc fingers and other domains cooperate in binding of *Drosophila* sry^b and sry^c proteins at specific chromosomal sites. Mol. Cell. Biol. *12*, 724–733.

Nüsslein-Volhard, C., Wieschaus, E., and Kluding, H. (1984). Mutations affecting the pattern of the larval cuticle in *Drosophila melanogaster* I. Zygotic loci on the second chromosome. Roux's Arch. Dev. Biol. *193*, 267–282.

Penton, A., Chen, Y., Staehling-Hampton, K., Wrana, J.L., Attisano, L., Szidonya, J., Cassill, J.A., Massagué, J., and Hoffmann, F.M. (1994). Identification of two bone morphogenetic protein type I receptors in Drosophila and evidence that Brk25D is a *decapentaplegic* receptor. Cell *78*, 239–250.

Perrimon, N. (1994). Signalling pathways initiated by receptor protein tyrosine kinases in *Drosophila*. Curr. Opin. Cell Biol. *6*, 260–266.

Perrimon, N., Engstrom, L., and Mahowald, A.P. (1989). Zygotic lethals with specific maternal effect phenotypes in *Drosophila melanogaster*. I. Loci on the X chromosome. Genetics *121*, 333–352.

Ramain, P., Heitzler, P., Haenlin, M., and Simpson, P. (1993). *pannier*, a negative regulator of *achaete* and *scute* in *Drosophila*, encodes a zinc finger protein with homology to the vertebrate transcription factor GATA-1. Development *149*, 1277–1291.

Ray, R.P., Arora, K., Nüsslein-Volhard, C., and Gelbart, W.M. (1991). The control of cell fate along the dorsal–ventral axis of the *Drosophila* embryo. Development *113*, 35–54.

Ring, J.M., and Martinez Arias, A. (1993). *puckered*, a gene involved in position-specific cell differentiation in the dorsal epidermis of the *Drosophila* larva. Development (Suppl.) *119*, 251–259.

Sambrook, S., Fritsch, E.I., and Maniatis, T. (1989). Molecular Cloning: A Laboratory Manual, Second Edition (Cold Spring Harbor, New York: Cold Spring Harbor Laboratory Press).

Seger, R., Ahn, N.G., Posada, J., Munar, E.S., Jensen, A.M., Cooper, J.A., Cobb, M.H., and Krebs, E.G. (1992). Purification and characterization of mitogen-activated kinase activator(s) from epidermal growth factor–stimulated A431 cells. J. Biol. Chem. *267*, 14373–14381.

Smith, D.B., and Johnson, K.S. (1988). Single-step purification of polypeptides expressed in *Escherichia coli* as fusions with glutathione S-transferase. Gene *67*, 31–40.

Terracol, R., and Lengyel, J.A. (1994). The *thick veins* gene of *Drosophila* is required for dorsoventral polarity of the embryo. Genetics *138*, 165–178.

Thummel, C.S., and Pirrotta, V. (1992). New pCaSpeR P element vectors. Dros. Inf. Serv. *71*, 150.

Tsuda, L., Inoue, Y.H., Yoo, M.A., Mizuno, M., Hata, M., Lim, Y.M., Adachi-Yamada, T., Ryo, H., Masamune, Y., and Nishida, Y. (1993). A protein kinase similar to MAP kinase activator acts downstream of the Raf kinase in Drosophila. Cell *72*, 407–414.

Valle, D., Kun, J., Linss, J., De Souza Garcia, E., Goldenberg, S. (1992). cDNA cloning and expression of *Rhodnius prolixus* vitellogenin. Insect Biochem. Mol. Biol. *23*, 457–465.

Wieschaus, E., and Nüsslein-Volhard, C. (1986). Looking at embryos. In *Drosophila*: A Practical Approach, D.M. Roberts, ed. (Oxford: IRL Press Limited), pp. 199–227.

Wieschaus, E., Nüsslein-Volhard, C., and Jürgens, G. (1984). Mutations affecting the pattern of the larval cuticle in *Drosophila melanogaster* III. Zygotic loci on the X-chromosome and the fourth chromosome. Roux's Arch. Dev. Biol. *193*, 296–307.

Winick, J., Abel, T., Leonard, M.W., Michelson, A.M., Chardon-Loriaux, I., Holmgren, R.A., Maniatis, T., and Engel, J.D. (1993). A GATA family transcription factor is expressed along the embryonic dorsoventral axis in *Drosophila melanogaster*. Development *119*, 1055–1065.

Yashar, B.M., Kelley, C., Yee, K., Errede, B., and Zon, L.I. (1993). Novel members of the mitogen-activated protein kinase activator family in *Xenopus laevis*. Mol. Cell. Biol. *13*, 5738–5748.

Young, P.E., Richman, A.M., Ketchum, A.S., and Kiehart, D.P. (1993). Morphogenesis in *Drosophila* requires nonmuscle myosin heavy chain function. Genes Dev. *7*, 29–41.

Zheng, C.F., and Guan, K.L. (1993). Properties of MEKs, the kinases that phosphorylate and activate the extracellular signal-regulated kinases. J. Biol. Chem. *268*, 23933–23939.

Zheng, C.F., and Guan, K.L. (1994). Activation of MEK family kinases requires phosphorylation of two conserved Ser/Thr residues. EMBO J. *13*, 1123–1131.

GenBank Accession Number

The accession number for the cDNA sequence reported in this paper is U05240.